Electron Spin Echo Envelope Modulation Spectroscopic Analysis of Altered Nitrogenase MoFe Proteins from *Azotobacter vinelandii*†

Victoria J. DeRose,‡ Chul-Hwan Kim,§ William E. Newton,§ Dennis R. Dean,*,§ and Brian M. Hoffman*,‡

Department of Chemistry, Northwestern University, Evanston, Illinois 60208, and Department of Biochemistry and Anaerobic Microbiology, Virginia Polytechnic Institute and State University, Blacksburg, Virginia 24061

Received September 12, 1994⊗

ABSTRACT: Electron spin echo envelope modulation (ESEEM) spectroscopy was used to study changes in the polypeptide environment of the FeMo-cofactor that were elicited by amino-acid substitutions within the nitrogenase MoFe protein α-subunit. A previous ESEEM study [Thomann *et al.* (1991) *Proc. Natl. Acad. Sci. U.S.A. 88,* 6620] detected modulation arising from nitrogen coupled to the $S = {}^3/_2$ spin system of the FeMo−cofactor (Fe_7S_9Mo:homocitrate). Such modulation was found to be sensitive to the substitution of α-195^{His} by α-195^{Asn} as indicated by whole-cell ESEEM analysis of mutant strains from *Azotobacter vinelandii.* Subsequent structural studies revealed that the α-195^{His} residue does not provide direct N-coordination to the cluster but is within hydrogen-bonding distance of one of a set of three sulfides that bridge the FeMo-cofactor subcluster fragments. In the present work, the ESEEM analysis is extended to both partially purified α-195^{Asn} MoFe protein and purified MoFe protein from an additional mutant strain in which α-195^{His} is replaced by α-195^{Gln}. The dramatic decrease in the intensity of the ESEEM signal resulting from the α-195^{Asn} substitution in whole cells was confirmed for the case of the isolated α-195^{Asn} MoFe protein. In contrast, substitution of α-195^{His} by α-195^{Gln} caused no detectable change in the modulation. Simulations of the α-195^{His} and α-195^{Gln} ESEEM data give quadrupole parameters of $e^2qQ = 2.2$ MHz and $\eta = 0.5$. Glutamine and histidine have similar chain lengths from the α-carbon to the protonated nitrogen that could provide a hydrogen bond to the FeMo-cofactor, whereas asparagine is shorter by one C−C bond and, therefore, cannot provide the putative hydrogen bond to the FeMo-cofactor under the constraints of the current structural models. However, simulations show that the ESEEM is quite sensitive to the electronic parameters of the ^{14}N nuclei, and therefore it is highly unlikely that an identical nitrogen modulation could arise from both an imidazole ring nitrogen provided by α-195^{His} and the glutamine amide group provided by α-195^{Gln}. Thus, these results indicate that the observed nitrogen modulation is not directly associated with the hydrogen bond provided by α-195^{His} but rather with the nitrogen moiety of a different residue whose proximity to the FeMo-cofactor is sensitive to certain substitutions at the α-195^{His} position. The ESEEM data, which provide a delicate probe of the local structure of the FeMo-cofactor, do however strongly suggest that either α-195^{His} or α-195^{Gln}, but not α-195^{Asn}, provides a hydrogen bond to FeMo-cofactor. This interpretation is in line with biochemical characterizations showing that both α-195^{His} and α-195^{Gln} MoFe proteins can bind N_2, whereas the α-195^{Asn} MoFe protein cannot. Thus, this information provides a correlation of phenotypic, biochemical, and spectroscopic properties of altered MoFe proteins produced by site-directed mutagenesis and should be useful in assigning mechanistic importance to specific structural features of the MoFe protein.

Nitrogenase catalyzes the biological reduction of dinitrogen to form ammonia: $N_2 + 8H^+ + 8e^- + 16MgATP \rightarrow 2NH_3 + H_2 + 16MgADP + 16P_i$. During catalysis, a nitrogenase component called the Fe protein transfers electrons to the MoFe protein component upon which is located the substrate binding site [see Dean *et al.* (1993) for a brief review]. Electron transfer is coupled to MgATP hydrolysis and component protein association−dissociation. The two metalloproteins that comprise nitrogenase have both recently been structurally characterized (Kim & Rees, 1992; Georgiadis *et al.*, 1992; Bolin *et al.*, 1993). The MoFe protein has an $\alpha_2\beta_2$-subunit structure, wherein each $\alpha\beta$-unit binds a unique Fe_8-S_{7-8} cluster, called the P-cluster pair, and an FeMo-cofactor (Fe_7S_9Mo:homocitrate). The site of substrate binding and reduction is generally agreed to be located at the FeMo-cofactor, which has been the subject of a multitude of biophysical studies [reviewed by Burgess (1990), Newton (1992)].

Current crystallographic modeling of FeMo-cofactor has provided the structure shown in Figure 1. The cluster is comprised of two partial cubes, one each of $MoFe_3S_3$ and Fe_4S_3 subclusters, that are joined by a ring of three sulfide bridges. FeMo-cofactor is anchored to the protein by an α-275^{Cys} thiolate ligand to Fe at one apex and by the δ-N of α-442^{His} to Mo at the opposite end. Other protein contacts may be provided by hydrogen-bonding interactions with amino-acid side chains that approach the cluster on all sides. An organic compound, homocitrate, is an additional constitu-

† This work was supported by the National Institutes of Health (HL13531, B.M.H.; DK37255, W.E.N. and D.R.D.; and a postdoctoral fellowship for V.J.D.), the USDA (93-37305-9623, B.M.H.), and the National Science Foundation (MCB 9207974, B.M.H.).

* To whom correspondence should be addressed.
‡ Northwestern University.
§ Virginia Polytechnic Institute and State University.

⊗ Abstract published in *Advance ACS Abstracts,* February 1, 1995.

0006-2960/95/0434-2809$09.00/0

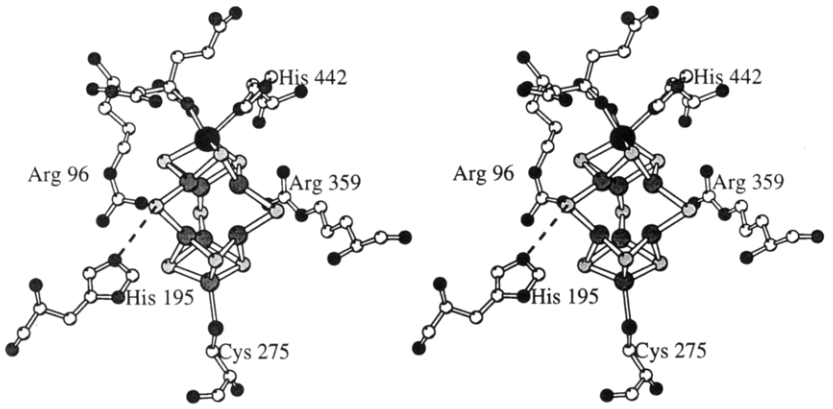

FIGURE 1: Stereoscopic view of FeMo-cofactor and selected residues in its environment. FeMo-cofactor is ligated to two protein residues, α-442^{His} and α-275^{Cys}. Also interacting closely with the cofactor are α-195^{His}, α-96^{Arg}, and α-359^{Arg}. An NH−S hydrogen bond of α-195^{His} to a bridging sulfide of the FeMo-cofactor is represented by a dashed line. The largest and darkest of the spheres is the Mo atom; the intermediate size spheres are Fe atoms, and the smallest and lightest spheres represent S atoms. A molecule of homocitrate, which provides two bonds to the Mo atom, is shown in the upper portion of the figure. In the homocitrate and protein components, C atoms are unshaded whereas the O and N atoms are the same, darker shade. The figure was generated with the program MOLSCRIPT (Kraulis, 1991) and kindly provided by S. Muchmore and J. Bolin, Purdue University.

ent of FeMo-cofactor (Hoover *et al.*, 1989) and provides two additional O ligands to the Mo atom. The Mo atom is, thus, coordinatively saturated with an S_3O_2N coordination sphere. The unusual structure of FeMo-cofactor invites speculation as to the mechanism of dinitrogen reduction [*e.g.*, Chan *et al.* (1993), Sellmann (1993)].

Placement of amino-acid substitutions within the FeMo-cofactor polypeptide environment by using site-directed mutagenesis has proven to be an effective method for identifying those residues that contribute to the catalytic and spectroscopic features of the MoFe protein [see, for example, Scott *et al.* (1990, 1992)]. In previous work, a series of residues was targeted by amino-acid sequence comparisons as potentially interacting with the metal cluster. As described in the preceding paper (Kim *et al.*, 1995), the substitution of one of these targeted residues, α-195^{His}, results in a number of interesting changes in catalytic properties of the enzyme. For example, substitutions at this position have been shown to induce (a) alteration in the electron distribution to products (C_2H_4 and H_2) and the generation of the new product, C_2H_6, during reduction of acetylene; (b) sensitivity of proton reduction to the presence of CO; (c) uncoupling of MgATP hydrolysis from electron transfer; and (d) perturbations in the $S = {}^3/_2$ EPR *g*-values and line shape. Of particular relevance to the present work, substitution of α-195^{His} by α-195^{Gln} results in an altered nitrogenase that is incapable of N_2 reduction but retains its ability to bind N_2. The latter property is demonstrated by the ability of N_2 to inhibit both acetylene and proton reduction. In contrast, substitution by α-195^{Asn} results in an altered MoFe protein that can neither bind nor reduce N_2 (Kim *et al.*, 1995).

Previous studies using the technique of electron spin echo envelope modulation (ESEEM) spectroscopy first identified N-modulation of the $S = {}^3/_2$ EPR signal of the wild-type enzyme from *Clostridium pasteurianum* (Thomann *et al.*, 1987). This modulation was assigned to the nitrogen of a ligand, most likely of a histidine residue, coupled to the EPR-active ($S = {}^3/_2$) state of the FeMo-cofactor. The ESEEM signal was further investigated in whole cells of *Azotobacter vinelandii* mutant strains in which various histidine residues had been substituted (Thomann *et al.*, 1991). The characteristic nitrogen modulation disappeared in an altered MoFe protein where α-195^{His} had been substituted by α-195^{Asn}, demonstrating a correlation between this signal, the α-195 residue, and the Nif$^-$ phenotype of the mutant organism. Modification of several other histidine residues caused no change in the nitrogen modulation. The ensuing model from crystallographic data, however, revealed that α-442^{His}, rather than α-195^{His}, provides the N ligand to Mo. The α-195^{His} residue is, however, within hydrogen-bonding distance of a bridging sulfide of the cluster (Figure 1).

In the present work, ESEEM spectra of altered nitrogenases from *A. vinelandii* having the α-195^{1His} position substituted by α-195^{Asn} and α-195^{Gln} were characterized in detail. Because N-modulation provides a convenient marker of local structural perturbations of the metallocluster environment, the goal of such studies is to correlate the ESEEM results both with the catalytic effects of such amino-acid substitutions and with structural features of FeMo-cofactor's polypeptide environment.

MATERIALS AND METHODS

Sample Preparation. Wild-type MoFe protein (α-195^{His}) and the altered MoFe protein produced by strain DJ540 (α-195^{Gln}) were isolated as previously described (Kim *et al.*, 1995). The altered MoFe protein produced by strain DJ528 (α-195^{Asn}) was partially purified using the same procedure as described for DJ540 MoFe protein except that the heat step and phenyl-Sepharose chromatography steps were omitted.

EPR and ESEEM Spectroscopy. EPR spectra shown here were obtained at 35 GHz (Q-band), on an instrument described previously (Werst *et al.*, 1991), as the low-temperature (2−4 K) dispersion-detected rapid-passage signal. Detection in this manner results in an absorptive line shape that closely approximates the integral of the derivative line shape obtained in traditional EPR data acquisition. ESEEM spectra were obtained on a pulsed EPR spectrometer operating at 9 GHz (X-band), described previously (Fan *et al.*, 1992). Data were obtained at a sample temperature of 2 K. ESEEM spectra were obtained with $\pi/2$ microwave pulses of 16 ns duration and powers of ~1 W, using the three-pulse "stimulated echo" sequence (Hahn, 1950; Mims & Peisach, 1979) that involves monitoring the electron spin echo amplitude as a function of time (T) between the second and third microwave pulses. Typical data traces consisted

of 256 points, with T beginning at 112 ns and stepped in increments of 44 ns. Other experimental parameters are given in the figure legends. Time-domain data were analyzed by Fourier transformation, using a modification of the procedure described by Mims (Mims, 1984) to eliminate "dead time" artifacts due to the nonzero start point.

ESEEM Simulations. Three-pulse "stimulated echo" ESEEM data were simulated using a program described in Cornelius *et al.* (1990), which takes into account contributions from selected molecular orientations in a powder pattern EPR signal. The ESEEM data depend on nuclear quadrupole parameters, the electron−nuclear hyperfine interaction, and the nuclear Zeeman interaction. In this simulation routine, the hyperfine interaction is treated as a combination of both an isotropic contribution and an anisotropic contribution that is modeled by a distance-dependent point−dipole approximation. Since the EPR signal from nitrogenase arises from an $S = {}^3/_2$ state, a true simulation requires consideration of the $S > {}^1/_2$ electronic spin. As previously discussed (True *et al.*, 1988; Venters *et al.*, 1986) for the case of nitrogenase, at a given g-value (g_{obs}) the measured nuclear hyperfine interactions are increased by factors of approximately $g_{obs}/2$. In addition, the nuclear Zeeman interaction [$\nu_N(^{14}N)$] is modified by a 'pseudonuclear Zeeman' term. In the simulations reported here, these effects were included in an approximate way by multiplying the intrinsic isotropic hyperfine value (reported as a_{int}) by a factor of $g_{obs}/2$ and by appropriately scaling $\nu_N(^{14}N)$.

RESULTS

The $S = {}^3/_2$ state of semireduced FeMo-cofactor has a rhombic EPR signal, arising from the $\pm{}^1/_2$ ground state Kramer's doublet, with observed g-values (g_1, g_2, g_3) = 4.33, 3.77, and 2.00. As previously reported (Kim *et al.*, 1995), the altered α-195^{Gln} MoFe protein does not exhibit a greatly perturbed $S = {}^3/_2$ EPR signal. In Figure 2, the EPR spectra of the altered α-195^{Asn} MoFe protein and the altered α-195^{Gln} MoFe protein are compared with MoFe protein from α-195^{His}. The g_1- and g_2-values show a slight rhombic shift to 4.36 and 3.64 in the α-195^{Gln} MoFe protein, while in the α-195^{Asn} MoFe protein an axial shift to 4.27 and 3.78 occurs, but the overall line shapes are effectively unchanged with respect to the wild-type MoFe protein. However, the intensity (per milligram of protein) of the EPR signal is substantially diminished in the α-195^{Asn} MoFe protein, which may indicate that it does not have a full complement of FeMo-cofactor (Kim *et al.*, 1995).

The technique of ESEEM spectroscopy has been used in a variety of biological systems to detect nuclei in the vicinity of an electronic spin (Mims & Peisach, 1981). Mixing of the nuclear sublevels induces modulations in the amplitude of an induced electron spin echo that is monitored as a function of timing between the pulses in an ESEEM pulse sequence. ESEEM is typically most sensitive to relatively weakly coupled nuclei and has been particularly useful in the case of weakly coupled ^{14}N nuclei, where the nuclear quadrupole interaction enhances sublevel mixing. The three-pulse 'stimulated echo' protocol used in this study eliminates common problems arising from short phase memories in metalloprotein samples (Mims & Peisach, 1979). The time-domain ESEEM patterns for wild-type (WT) and mutant MoFe proteins, obtained at a field position corresponding

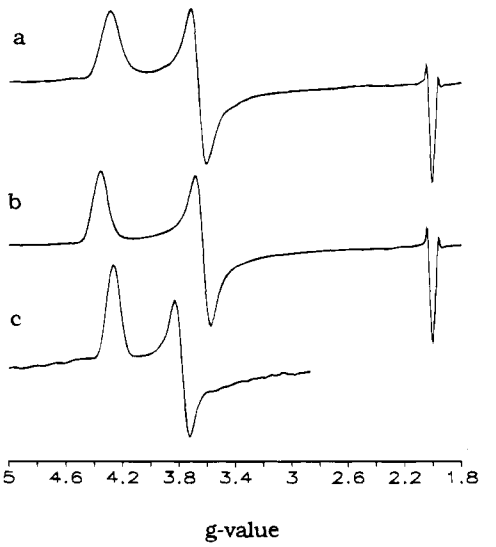

FIGURE 2: Continuous wave EPR of nitrogenase α-195^{His}-substituted MoFe proteins isolated from *A. vinelandii* mutant strains. EPR spectra are shown for the (a) α-195^{His} MoFe protein and mutant (b) α-195^{Gln} and (c) α-195^{Asn} MoFe proteins. Spectra are plotted as the numerical derivative and as a function of g-value. The $g \sim 2$ region of spectrum c is not shown due to contamination by $g_{av} \sim 1.94$ Fe protein. Spectra were obtained using dispersion detection with 100 kHz field modulation, at sample temperatures of 2 K, and the following conditions: 2 G amplitude field modulation, 5 mW microwave power, and (a) 35.026, (b) 35.148, and (c) 35.117 GHz.

to $g_2 = 3.8$, are shown in Figure 3a−c. These data reveal a complex pattern of modulation arising from ^{14}N coupled to the electronic spin of the FeMo-cofactor. Figure 3d−f displays the Fourier transforms of the time-domain traces. At this g-value, the α-195^{His} and α-195^{Gln} proteins give indistinguishable traces, with the Fourier-transformed data indicating modulation frequencies of 0.7, 1.4, 2.1, and 3.6 MHz. Several smaller amplitude peaks are also evident. The ESEEM data shown here for the purified α-195^{His} MoFe protein (Figure 3a,d) appear essentially identical to those previously reported for both purified wild-type MoFe protein (Thomann *et al.*, 1987) and whole cells of wild-type *A. vinelandii* (Thomann *et al.*, 1991).

Substitution of α-195^{His} by α-195^{Asn} results in a dramatic attenuation of the ESEEM (Figure 3b). Likewise, there is a loss in intensity of the major peaks in the Fourier-transformed data (Figure 3e), most strikingly seen for the 1.4 MHz peak. It should be noted that the decrease in the ESEEM observed for the α-195^{Asn} MoFe protein cannot be accounted for by a relatively lower EPR signal, since the accumulated electron spin echo signal intensities shown in Figure 3 are all roughly equal. As previously determined by work with whole cells (Thomann *et al.*, 1991), it is apparent that the α-195^{Asn} MoFe protein has lost an interaction between a nitrogen nucleus and the electronic spin of the cofactor. The data obtained on the partially purified α-195^{Asn} MoFe protein (Figure 3b) do exhibit a weak residual modulation which appears as low amplitude peaks in the Fourier transform.

Figure 3d,f shows that the ESEEM data collected at $g = 3.77$ from the altered α-195^{Gln} MoFe protein and the wild-type α-195^{His} MoFe protein are identical. However, for a nonisotropic EPR signal, data collected at multiple magnetic fields are required to fully characterize a nucleus coupled to a paramagnetic center [reviewed in Hoffman *et al.* (1993)]. In collecting such data, it was found that data collected at $g = 4.3$ show particularly deep modulation. Figure 4 displays

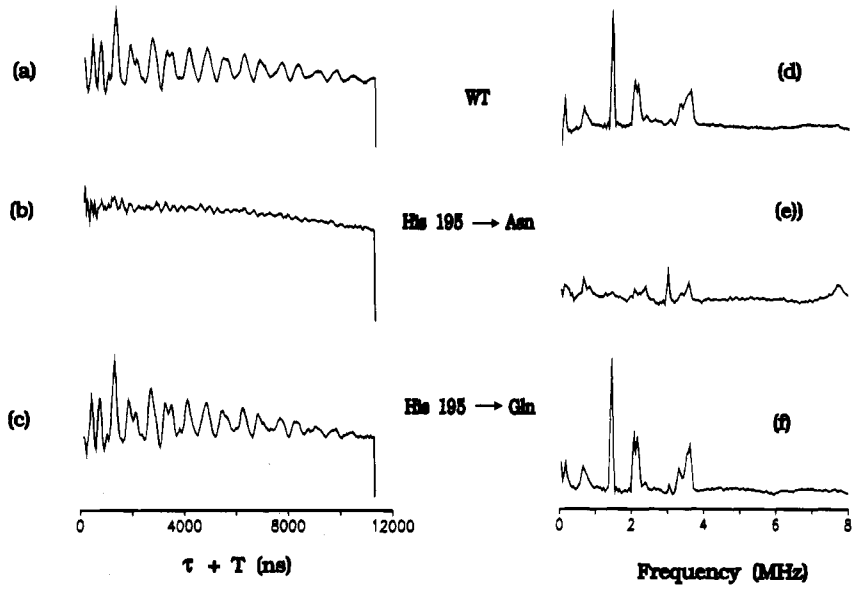

FIGURE 3: ESEEM spectra at $g = 3.8$ of wild-type α-195^{His} and α-195^{Gln} MoFe proteins. The time-domain traces (a−c) of the amplitude of the stimulated electron spin echo following a three-pulse sequence, obtained at $g = 3.8$, are shown with the accompanying Fourier transforms (d−f). Envelope modulation assigned as the interaction of a ^{14}N nucleus with the $S = {}^3/_2$ spin state of the FeMo-cofactor cluster is evident in data taken on (a, d) α-195^{His} (wild-type) MoFe protein and (c, f) α-195^{Gln} MoFe protein but is markedly diminished in (b, e) α-195^{Asn} MoFe protein. Instrument conditions: $\tau = 132$ ns; (a) 1790 G, 9.432 GHz, average of 480 transients; (b) 1800 G, 9.526 GHz, average of 960 transients; (c) 1790 G, 9.455 GHz, average of 240 transients. Other conditions are as described in the text under Materials and Methods.

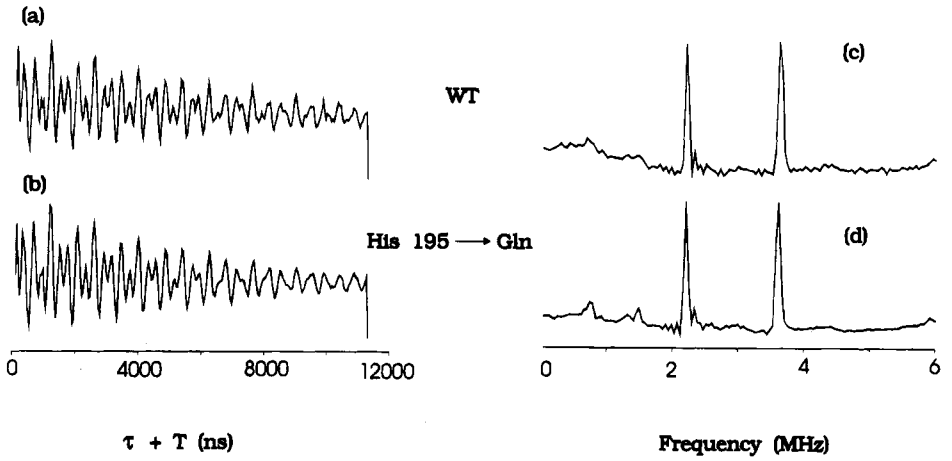

FIGURE 4: ESEEM spectra at $g = 4.3$ of α-195^{His} and α-195^{Gln} MoFe proteins. The time-domain traces (a, b) and Fourier transforms (c, d) of three-pulse ESEEM data obtained at $g = 4.3$ are shown, displaying identical modulation from the α-195^{His} MoFe protein (wild-type, upper traces) and the α-195^{Gln} MoFe protein (lower traces). Instrument conditions: $\tau = 152$ ns; 1560 G; (a) 9.432 GHz, average of 320 transients; (b) 9.455 GHz, average of 600 transients. Other conditions are described in the text under Materials and Methods.

data obtained at $g_1 = 4.3$ for both α-195^{His} and α-195^{Gln} MoFe proteins. The Fourier transform of the modulation at this g-value yields two very sharp peaks at 2.2 and 3.6 MHz and two broad, low-amplitude peaks at frequencies <2 MHz. These data also are identical for the two proteins, and so it can be concluded that substitution of α-195^{His} by α-195^{Gln} causes no changes in the FeMo cofactor ESEEM.

Simulations were performed in order to establish the sensitivity of the ESEEM at $g = 3.8$ and 4.3 to the nuclear quadrupole parameters e^2qQ and η (Figure 5). The ESEEM patterns obtained at the two g-values differ dramatically because the measurements sample different sets of orientations of the protein with respect to the external magnetic field (Cornelius *et al.*, 1990; Flanagan & Singel, 1987). In particular, ESEEM data obtained at $g_2 = 3.8$ arise from a set of many different molecular orientations that contribute to intensity at the middle of the EPR envelope, whereas data obtained at $g_1 = 4.3$ arise from a 'single-crystal-like' position, near the edge of the EPR envelope, where the majority of the centers that contribute to the EPR signal have the external field oriented along the $g = 4.3$ axis of the molecular g-tensor. As seen in Figure 5, the patterns at both g-values (Figure 5a,e) are simulated quite well (Figure 5b,f), using the parameters of $a_{int} = 1$ MHz, $e^2qQ = 2.2$ MHz, $\eta = 0.5$, and a point−dipole distance of 4 Å (see Methods). In particular, the frequencies of the two sharp peaks in the Fourier transform of ESEEM data obtained at $g = 4.3$ are matched well in the simulation shown in Figure 5f. Even very small variations in the NQI parameters result in detectable perturbations of the simulated data. This is demonstrated in Figure 5c,g, which displays the effects of modifying the values of the NQI parameters only slightly [$(e^2qQ, \eta) = (2.4, 0.7)$], and in Figure 5d,h, with values more similar to the amino nitrogen of a histidine ring [$(e^2qQ, \eta) = (1.4, 0.9)$] (Ashby *et al.*, 1978).

Table 1: Selected Nuclear Quadrupole Parameters

compound	e^2qQ (MHz)	η	reference
MoFe protein	2.2	0.5	this work
histidine (amino)	1.4	0.91	Ashby et al. (1978)
histidine (imino, unbound)	3.4	0.13	Ashby et al. (1978)
histidine (imino, bound to metal ion)	1.9−2.8	0.69−0.25	Ashby et al. (1978)
asparagine (amido)	2.5	0.39	Hunt and Mackay (1974)
diglycine (peptide amido)	3.0	0.41	Edmonds and Speight (1971)

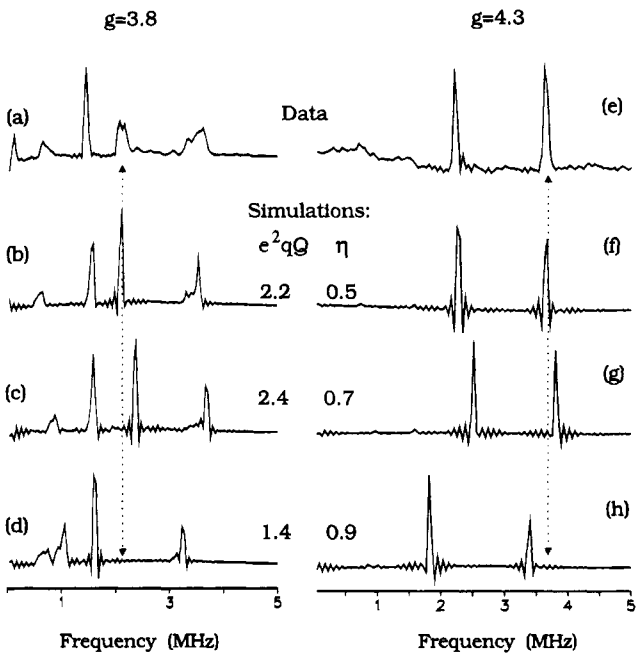

FIGURE 5: Comparison of real and simulated ESEEM data for wild-type α-195^{His} MoFe protein. The Fourier transforms of α-195^{His} MoFe protein ESEEM data obtained at $g = 3.8$ (a) and $g = 4.3$ (e) are shown in comparison with simulations performed as described under Materials and Methods. The data are simulated with ^{14}N hyperfine values of $a_{int} \sim 1$ MHz and $R = 4$ Å and the following values for e^2qQ (MHz) and η: 2.2, 0.5 (b, f); 2.4, 0.7 (c, g); and 1.4, 0.9 (d, h). Simulations b and f compare well with the experimental data, and the other traces demonstrate the sensitivity of the simulations to perturbations of the quadrupole parameters.

DISCUSSION

Glutamine and histidine have similar chain lengths between the α-carbon and the protonated nitrogen (the amide nitrogen and the imidazole ϵ-nitrogen, respectively) that could provide a hydrogen bond to a central sulfide of the FeMo-cofactor. Asparagine is shorter by one C−C bond and so is less likely to form this putative hydrogen bond. These structural features in principle could explain the loss of modulation in the α-195^{Asn} MoFe protein and its presence in both the α-195^{His} and α-195^{Gln} MoFe proteins. However, as discussed below, the fact that the ^{14}N-modulation is identical for both of the latter proteins makes it extremely unlikely that residue-195 provides the ^{14}N nucleus that is responsible for the modulation.

The interactions giving rise to ESEEM from a given nucleus include both the hyperfine interaction, which reflects the distribution of the unpaired electronic spin, and the nuclear electric quadrupole interaction (NQI) parameters, which reflect the bonding interactions of that atom. The NQI properties are conveniently described by the parameters e^2qQ and η, where e^2qQ is the magnitude of the electric field gradient for a defined z-direction at the nucleus and η describes the charge asymmetry normal to that direction. Changes in electronic properties are sensitively reflected by changes in one or both parameters [reviewed in Edmonds (1977)]. The measured NQI parameters for the nonbonding, amino nitrogen of imidazole are 1.4 MHz and 0.9 for e^2qQ and η, respectively (Ashby *et al.*, 1978) (listed in Table 1). These values can be contrasted with those values of 2.5 MHz and 0.4 that are measured for the amido group of asparagine (Hunt & Mackay, 1974) and which presumably represent glutamine as well. Hydrogen bonding is expected in both cases to alter the ^{14}N NQI parameters. The measured values of e^2qQ and η for the imino nitrogen of nonbonded imidazole are ~3.4 MHz and 0.1, respectively, whereas bonding of that nitrogen to a metal atom reduces e^2qQ and raises η in a manner proportional to the reduced occupancy of the bonding nitrogen p-orbital (Ashby *et al.*, 1978).

As shown in Figure 5, simulations indicate that the nitrogenase ESEEM is very sensitive to changes in these parameters. For the ESEEM data collected on α-195^{His} and α-195^{Gln} MoFe proteins to be indistinguishable strongly suggests that the nucleus giving rise to the modulation has exactly the same NQI parameters in each case. Consideration of the reference quadrupole parameters (Table 1) shows that it is highly unlikely that this requirement could be fulfilled by the nitrogen of the amide group of glutamine and the amino nitrogen of histidine. Indeed, one would require H-bonding to shift the quadrupole parameters for Gln and His in different directions by widely different amounts, and to do so with exquisite precision, in order to achieve identical NQI values. Thus, it must be concluded that the ESEEM of MoFe protein arises from a moiety other than α-195^{His}.

One alternative could be that the observed nitrogen modulation arises from a coordinated histidine, as was initially proposed (Thomann *et al.*, 1987, 1991). The quadrupole parameters for a metal-coordinated imidazole N atom of His (Ashby *et al.*, 1978) are consistent with such an assignment (Table 1). The crystal structure identified α-442^{His} as coordinated, through its Nδ1 atom, to the Mo atom of FeMo-cofactor. The available experimental evidence does not directly eliminate the possibility that the α-195^{Asn} substitution affects α-442^{His} coordination to the Mo. However, because His is a strong donor ligand to metals, it seems improbable that substitution of α-195^{His} by α-195^{Asn} could effect displacement of α-442^{His} from the Mo atom, particularly at a significant distance (~5 Å) 'across' the cluster. Moreover, the α-195^{Asn} MoFe protein is unlikely to have gross changes in either the structure of the FeMo-cofactor or its polypeptide environment because the $S = {}^3/_2$ EPR spectrum does not show large changes in line shape or g-value when compared to the wild-type MoFe protein (Figure 2). In addition, the α-195^{Asn} MoFe protein is able to reduce both acetylene and protons, albeit at reduced rates, and thus its substrate reduction site must be sufficiently intact to effect these reactions (Kim *et al.*, 1995). Finally, substitution of α-442^{His} by α-442^{Asn} results in an altered MoFe protein that exhibits neither catalytic activity nor an

$S = {}^3/_2$ EPR spectrum (J. Peters, W. Newton, and D. Dean, unpublished).

The current structural information indicates that the MoFe cofactor interacts with a network of other NH−S bonds provided by the protein through peptide nitrogens and, in particular, by two strictly conserved arginine residues, α-96^{Arg} and α-359^{Arg} (Figure 1). These residues are obvious candidates as the source of the MoFe protein nitrogen ESEEM. The NQI parameters that have been reported for the amide nitrogens in poly(glycine) of $e^2qQ \sim 3.0$ MHz and $\eta \sim 0.4-0.8$ (Edmonds & Speight, 1971) are higher than the values of $e^2qQ \sim 2.2$ MHz and $\eta \sim 0.5$ that are derived from preliminary simulations of the nitrogenase ESEEM data (Figure 5), although the amide NQI parameters may be expected to change with hydrogen-bonding interactions. The proximity of the potential α-96^{Arg} NH−S bond to the FeMo-cofactor (Figure 1) makes this residue an attractive choice. To our knowledge, however, no NQI parameters for arginine have been reported. Our preliminary mutagenesis results show that an *A. vinelandii* strain which produces an altered MoFe protein where α-96^{Arg} is substituted by α-96^{Gln} remains capable of slow diazotrophic growth. In contrast, substitution of α-359^{Arg} by α-359^{Gln} eliminates diazotrophic growth and nitrogenase activity, whereas substitution by α-359^{Lys} results in moderate diazotrophic growth and significant nitrogenase activity (K. Thrasher, D. Dean, and W. Newton, unpublished). Thus, ESEEM analysis of these altered MoFe proteins should reveal whether either α-96^{Arg} or α-359^{Arg} contributes to the observed N-modulation.

The results reported here show that ESEEM provides a remarkably sensitive spectroscopic probe for small structural rearrangements induced by substituting amino acids located within the FeMo-cofactor environment. Biochemical studies of both the α-195^{Gln} MoFe protein and the wild-type MoFe protein show that the reduction of both protons and acetylene is inhibited by N_2, whereas proton and acetylene reduction catalyzed by the α-195^{Asn} MoFe protein is not inhibited by N_2 (Kim *et al.*, 1995). These observations lead to the conclusion that the α-195^{Gln} MoFe protein, but not the α-195^{Asn} MoFe, retains the capacity to bind N_2. One rationale for these observations is that the α-195^{Gln} residue is able to provide a NH−S hydrogen bond to the FeMo-cofactor, as proposed for the α-195^{His} residue (see Figure 1). This substitution, therefore, would probably result in minimal disruption of the structure around the FeMo-cofactor in the α-195^{Gln} MoFe protein. The corollary, that the shorter chain length of the α-195^{Asn} residue disrupts the potential NH−S interaction, appears to be supported by the inability of α-195^{Asn} MoFe protein to bind N_2. The present ESEEM results correlate with the catalytic properties of the altered MoFe proteins in that an NH−S bond provided by the α-195^{His} position appears necessary for both N-modulation recognized by ESEEM and N_2 binding, although we have shown it to be unlikely that the nitrogen ESEEM arises from the α-195 residue. Our interpretation of these results is that the NH−S hydrogen bond provided by α-195^{His} contributes to the "correct" orientation of FeMo-cofactor within the polypeptide matrix and that this orientation is essential for formation of another NH−S bond that is observed spectroscopically. Although not yet proven generally, the present data also suggest that N-modulation of the $S = {}^3/_2$ EPR signal may be a signature of the ability of a MoFe protein to bind N_2.

ACKNOWLEDGMENT

We thank Prof. John McCracken for providing an ESEEM simulation routine and for helpful discussions, Prof. Jeff Bolin for providing detailed structural information, and Mr. Clark E. Davoust and Dr. Peter Doan for technical assistance.

REFERENCES

Ashby, C. I., Cheng, C. P., & Brown, T. L. (1978) *J. Am. Chem. Soc. 100*, 6057−6063.

Bolin, J. T., Campobasso, N., Muchmore, S. W., Morgan, V. T., & Mortenson, L. E. (1993) in *Molybdoenzymes, cofactors and model systems* (Steifel, E., Coucouvanis, D., & Newton, W. E., Eds.) pp 186−195, American Chemical Society, Washington, DC.

Burgess, B. K. (1990) *Chem. Rev. 90*, 1377−1406.

Chan, M. K., Kim, J. S., & Rees, D. C. (1993) *Science 260*, 792−794.

Cornelius, J. B., McCracken, J., Clarkson, R. B., Belford, R. L., & Peisach, J. (1990) *J. Phys. Chem. 94*, 6977−6982.

Dean, D. R., Bolin, J. T., & Zheng, L. (1993) *J. Bacteriol. 175*, 6737−6744.

Edmonds, D. T. (1977) *Phys. Lett. 29C*, 233−290.

Edmonds, D. T., & Speight, P. A. (1971) *Phys. Lett. 34A*, 325−326.

Fan, C. L., Doan, P. E., Davoust, C. E., & Hoffman, B. M. (1992) *J. Magn. Reson. 98*, 62−72.

Flanagan, H. L., & Singel, D. J. (1987) *J. Chem. Phys. 87*, 5606−5616.

Georgiadis, M. M., Komiya, H., Chakrabarti, P., Woo, D., Kornuc, J. J., & Rees, D. C. (1992) *Science 257*, 1653−1659.

Hahn, E. L. (1950) *Phys. Rev. 80*, 580−594.

Hoffman, B. M., DeRose, V. J., Doan, P. E., Gurbiel, R. J., Houseman, A. L. P., & Telser, J. (1993) in *Biological Magnetic Resonance* (Berliner, L. J., & Reuben, J., Eds.) Vol. 13, pp 151−217, Plenum Press, New York.

Hoover, T. R., Imperial, J., Ludden, P. W., & Shah, V. K. (1989) *Biochemistry, 28*, 2768−2771.

Hunt, M. J., & Mackay, A. L. (1974) *J. Magn. Reson. 15*, 402−414.

Kim, J., & Rees, D. C. (1992) *Nature (London) 360*, 553−560.

Kim, C.-H., Newton, W. E., & Dean, D. R. (1995) *Biochemistry 34*, 2798−2808.

Kraulis, P. (1991) *J. Appl. Crystallogr. 24*, 946−950.

Mims, W. B. (1984) *J. Magn. Reson. 59*, 291−306.

Mims, W. B., & Peisach, J. (1979) *J. Biol. Chem. 254*, 4321−4323.

Mims, W. B., & Peisach, J. (1981) in *Biological Magnetic Resonance* (Berliner, L. J., & Reuben, J., Eds.) Vol. 3, pp 213−263, Plenum, New York.

Newton, W. E. (1992) in *Biological Nitrogen Fixation* (Stacey, G., Burris, R. H., & Evans, H. J., Eds.) pp 877−929, Chapman and Hall, New York.

Scott, D. J., May, H. D., Newton, W. E., Brigle, K. E., & Dean, D. R. (1990) *Nature 343*, 188−190.

Scott, D. J., Dean, D. R., & Newton, W. E. (1992) *J. Biol. Chem. 267*, 20002−20010.

Sellmann, D. (1993) *Angew. Chem., Int. Ed. Engl. 32*, 64−67.

Thomann, H., Morgan, T. V., Jin, H., Burgmayer, S. J. N., Bare, R. E., & Stiefel, E. I. (1987) *J. Am. Chem. Soc. 109*, 7913−7914.

Thomann, H., Bernardo, M., Newton, W. E., & Dean, D. R. (1991) *Proc. Natl. Acad. Sci. U.S.A. 88*, 6620−6623.

True, A. E., Nelson, M. J., Venters, R. A., Orme-Johnson, W. H., & Hoffman, B. M. (1988) *J. Am. Chem. Soc. 110*, 1935−1943.

Werst, M., Davoust, C. E., & Hoffman, B. M. (1991) *J. Am. Chem. Soc. 113*, 1533−1538.

Venters, R. A., Nelson, M. J., McLean, P. A., True, A. E., Levy, M. A., Hoffman, B. M., & Orme-Johnson, W. H. (1986) *J. Am. Chem. Soc. 108*, 3487−3498.

BI942151I